Particle flow stability in tubular fluidized bed solar receivers

Guillaume Sahuquet, Ronny Gueguen, Samuel Mer, Adrien Toutant, Françoise Bataille, Gilles Flamant

Particle flow stability in tubular fluidized bed solar receivers

Guillaume Sahuquet [1], Ronny Gueguen [1], Samuel Mer [2, a], Adrien Toutant [2, a], Françoise Bataille [2, b], Gilles Flamant [3]

[1] PhD student, PROMES-CNRS, 7 rue du Four solaire, 66120 Odeillo, France. +33(0) 4 68 30 77 00
[2] Dr., [a] Ass. Prof., [b] Prof., PROMES-CNRS, Rambla de la Thermodynamique, Tecnosud, 66100 Perpignan, France. +33(0) 4 68 68 22 22
[3] corresponding author, Dr., Senior CNRS Researcher, PROMES-CNRS (UPR 8521), 7 rue du Four solaire, 66120 Odeillo, France, +33(0) 4 68 30 77 58, Gilles.Flamant@promes.cnrs.fr

1. Introduction and experimental setup

Concentrating solar power (CSP) is a promising technology currently undergoing brisk development [1]. Among CSP systems, solar towers have the potential to generate power efficiently [2]. Molten salt is the commonly used heat transfer fluid (HTF) [3], but solar salt has limited operating temperatures which decrease the efficiency of the power block. To overcome this issue and reduce costs, new particle receivers are under development worldwide as the falling particle receiver of Sandia National Laboratories, the centrifugal receiver of the German Aerospace Center and the fluidized particle-in-tube of the french National Center for Scientific Research [4].
The European project Next-CSP aims to use solid-gas fluidized bed as HTF in tubular solar receivers. The material chosen is olivine [5] with a Sauter diameter of 30.0 µm (group A of the Geldart classification) that permits to reach high temperatures, up to 800°C and more. This temperature level allows the use of a combined Brayton-Rankine thermodynamic and s-CO_2 cycles with a 50 % efficiency. A pilot-scale test unit is currently under construction at Thémis, France, while a smaller cold mock-up was constructed to study the hydrodynamics of the particle suspension flow at PROMES laboratory.
Figure 1 shows a schematic (a) and a 3D (b) representation of the cold mock-up. The particles are fluidized in a dispenser thanks to a homogeneously distributed air flowrate. By applying pressure into the dispenser with a pressure-control valve, the fluidized bed passes into a 3m-long transparent glass tube of 4.5 cm internal diameter and is collected in a fluidized bed collector, creating a particle flowrate G_P measured by a weighing device. A secondary air flowrate q_{ae} is applied at an injection nozzle of diameter d_{ae} at the bottom of the tube.
Depending on the values of q_{ae} and G_P, the particle flow is either stable or unstable. When an instability occurs the total pressure in the dispenser decreases and there are significant variations of the particle flowrate. This paper is focused on the conditions of occurrence of this instability that can result, in the solar application, in an emergency stop of the power plant and aims to define a stability diagram of the particle flow in order to define the best operating conditions for the full-scale unit.

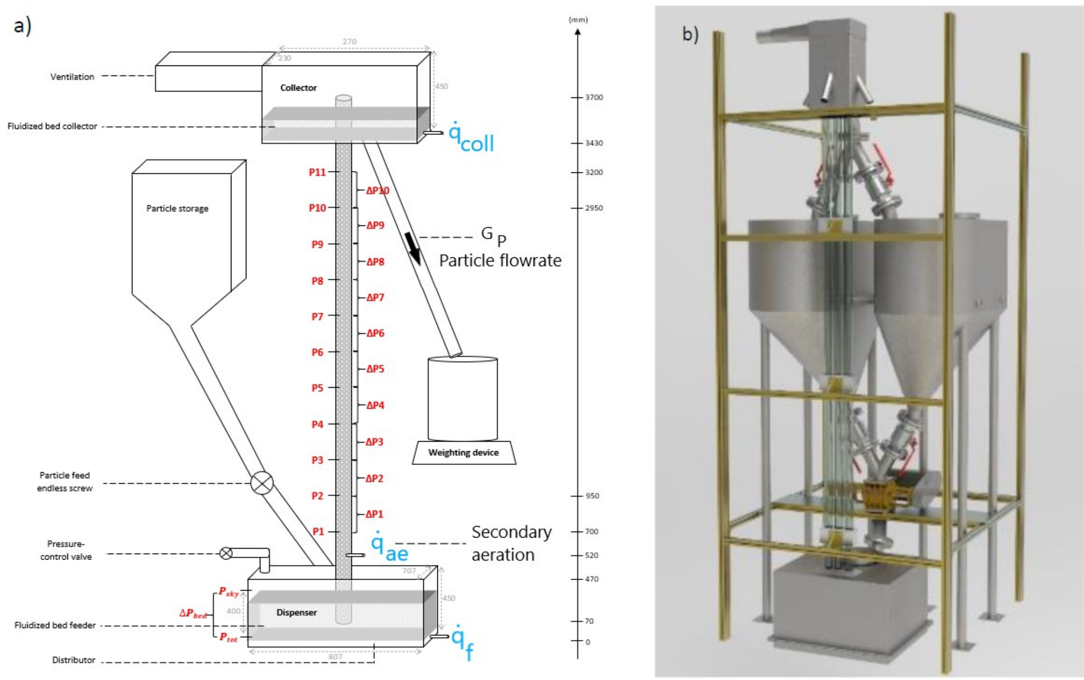

Fig. 1: Schematic representation of the cold mock-up (a), and 3D view (b).

2. Results and discussion

The stability of the particle flow as a function of the secondary air flowrate q_{ae} (in Nm^3/s) and of the solid flowrate G_P (in $kg/(m^2.s)$) is studied.
Firstly, the particle flow is always unstable without aeration.
Secondly, two specific values of q_{ae} and one caracteristic value of G_P delimit two main domains (Fig. 2):

- For values of q_{ae} under a threshold air flowrate called $q_{unstable}$, the mass flow is unconditionally unstable whatever the value of G_P . This domain represents the unstable area.
- For values of q_{ae} above a threshold air flowrate called q_{stable} , the particle flow is unconditionally stable whatever the value of G_P . This domain represents the stable area.

For values of q_{ae} between $q_{unstable}$ and q_{stable} , the mass flow is either stable or unstable depending on the value of G_P. The boundary between these two states follows a sigmoid curve. This domain is called transition area.

The unconditionally stable area is splitted into two sub-areas :

- For small values of G_P (under a certain value $G_p^{transition}$), where the fluidized bed gets denser with the height in the tube (i.e. the partial derivative of the solid volume fraction with respect to the height is positive);
- For high particle flowrate (G_P above $G_p^{transition}$), where the fluidized bed dilutes with the height (i.e. the partial derivative of the solid volume fraction with respect to the height is negative).

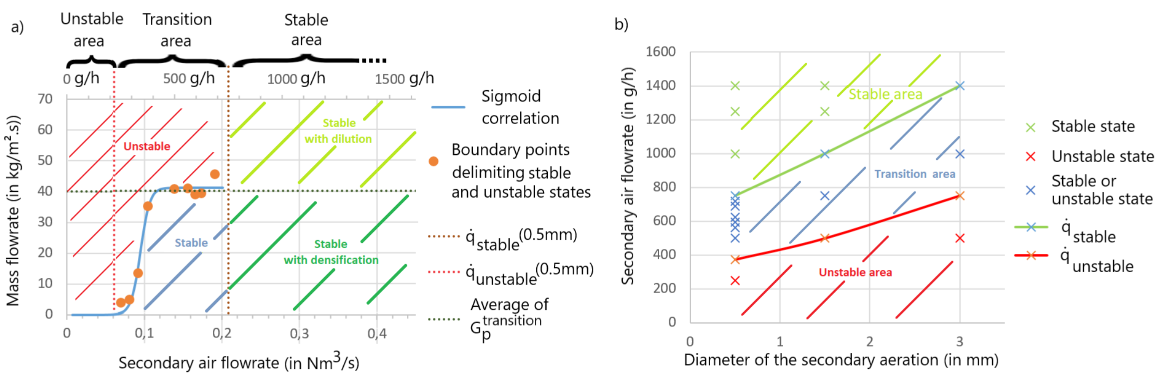

Fig. 2: a) Stability diagram in function of q_{ae} and G_P. b) Stability diagram in function of d_{ae} and q_{ae} .

Figure 2.a represents these four domains for a nozzle's diameter of the secondary aeration d_{ae} of 0.5 mm. These experimental data show that a secondary aeration at the bottom of the tube is a necessary condition to get a stable particle flow and that the aeration flowrate must overcome a given threshold to reach unconditional particle flow stability. The latter caracteristic is essential for the solar application.
In addition, the boundaries of these domains depend on the nozzle's diameter d_{ae} of the secondary aeration, with an increase of q_{stable} and $q_{unstable}$ with d_{ae} (Fig.2.b), but with no influence on $G_p^{transition}$.
For our tested diameters, the thinner the nozzle's diameter the smaller the air flowrate necessary to get unconditional stability. In fact, the sigmoid tends to be left shifted with the reduction of the nozzle's diameter.
In the final paper, more experimental data would be presented and discussed.

Acknowledgements

Next-CSP is a project that has received funding from the European Union's Horizon 2020 research and innovation program under grant agreement No. 727762.

References

[1] Barlev D., Vidu R., Stroeve P., 2011. Innovation in concentrated solar power.
Solar Energy Materials and Solar Cells 95(10), p. 2703-2725. DOI: 10.1016/j.solmat.2011.05.020
[2] Behar O., Khellaf A., Mohammedi K., 2013. A review of studies on central receiver solar thermal power plants.
Renewable and Sustainable Energy Reviews 23, p. 12-39. DOI: 10.1016/j.rser.2013.02.017
[3] Tyner C., Wasyluk D., 2014. eSolar’s Modular, Scalable Molten Salt Power Tower Reference Plant Design.
Energy Procedia 49, p. 1563-1572. DOI: 10.1016/j.egypro.2014.03.165
[4] Ho C., 2016. A review of high-temperature particle receivers for concentrating solar power.
Applied Thermal Engineering 109, p. 958-969. DOI: 10.1016/j.applthermaleng.2016.04.103
[5] Kang Q., Flamant G., Dewil R., Baeyens J., Zhang H.L., Deng Y.M., 2019. Particles in a circulation loop for solar energy capture and storage. Particuology 43, p. 149-156. DOI: 10.1016/j.partic.2018.01.009